

to appear in ApJ

Five Intermediate-Period Planets from the N2K Sample ^{1,2}

Debra A. Fischer³, Steven S. Vogt⁴, Geoffrey W. Marcy⁵, R. Paul Butler⁶, Bun'ei Sato⁷,
 Gregory W. Henry⁸, Sarah Robinson⁴, Gregory Laughlin⁴, Shigeru Ida⁷, Eri Toyota⁹
 Masashi Omiya¹⁰ Peter Driscoll¹¹, Genya Takeda¹², Jason T. Wright⁵, John A. Johnson⁵

fischer@stars.sfsu.edu

ABSTRACT

We report the detection of five Jovian mass planets orbiting high metallicity stars. Four of these stars were first observed as part of the N2K program and exhibited low RMS velocity scatter after three consecutive observations. However, follow-up observations over the last three years now reveal the presence of

¹Based on observations obtained at the W. M. Keck Observatory, which is operated by the University of California and the California Institute of Technology. Keck time has been granted by NOAO and NASA.

²Based on observations obtained at the Subaru Telescope, which is operated by the National Astronomical Observatory of Japan

³Department of Physics & Astronomy, San Francisco State University, San Francisco, CA 94132; fischer@stars.sfsu.edu

⁴UCO/Lick Observatory, University of California at Santa Cruz, Santa Cruz, CA 95064

⁵Department of Astronomy, University of California, Berkeley, CA USA 94720

⁶Department of Terrestrial Magnetism, Carnegie Institute of Washington DC, 5241 Broad Branch Rd. NW, Washington DC, USA 20015-1305

⁷Tokyo Institute of Technology, 2-12-1 Okayama, Meguro-ku, Tokyo 152-8550, Japan

⁸Center of Excellence in Information Systems, Tennessee State University, 3500 John A. Merritt Blvd., Box 9501, Nashville, TN 37209

⁹Department of Earth and Planetary Sciences, Graduate School of Science, Kobe University, 1-1 Rokkodai, Nada, Kobe 657-8501, Japan

¹⁰Department of Physics, Tokai University, 1117 Kitakaname, Hiratsuka, Kanagawa 259-1292, Japan

¹¹Department of Earth and Planetary Sciences, Johns Hopkins University, Baltimore, MD 21218

¹²Department of Physics and Astronomy, Northwestern University, 2145 Sheridan Road, Evanston, IL 60208

longer period planets with orbital periods ranging from 21 days to a few years. HD 11506 is a G0V star with a planet of $M \sin i = 4.74 M_{\text{JUP}}$ in a 3.85 year orbit. HD 17156 is a G0V star with a $3.12 M_{\text{JUP}}$ planet in a 21.2 day orbit. The eccentricity of this orbit is 0.67, one of the highest known for a planet with a relatively short period. The orbital period for this planet places it in a region of parameter space where relatively few planets have been detected. HD 125612 is a G3V star with a planet of $M \sin i = 3.5 M_{\text{JUP}}$ in a 1.4 year orbit. HD 170469 is a G5IV star with a planet of $M \sin i = 0.67 M_{\text{JUP}}$ in a 3.13 year orbit. HD 231701 is an F8V star with planet of $1.08 M_{\text{JUP}}$ in a 142 day orbit. All of these stars have supersolar metallicity. Three of the five stars were observed photometrically but showed no evidence of brightness variability. A transit search conducted for HD 17156 was negative but covered only 25% of the search space and so is not conclusive.

Subject headings: planetary systems – stars: individual (HD 11506, HD 17156, HD 125612, HD 170469, HD 231701)

1. Introduction

Ongoing Doppler surveys of stars closer than 150 pc have detected more than 200 exoplanets (Butler et al. 2006, Wright et al. 2007). This ensemble of exoplanets exhibit a diverse range of statistical characteristics (Marcy et al. 2005). Notably, the mass distribution of exoplanets falls exponentially for masses greater than one Jupiter-mass. In addition, there is a statistical pile-up of planets in orbits of just a few days, a paucity of planets with periods between 10 - 100 days, and a rising number of gas giant planets found at separations greater than 1 AU. Orbital eccentricities span a surprising range from 0 - 0.93, although 92% of planet eccentricities are less than 0.6 and even for planets with periods longer than five days (i.e., not tidally circularized) the median exoplanet eccentricity is 0.26.

It has also been shown that planet formation is tied to the chemical composition of the host star. There is a few percent probability of finding a gas giant planet around a solar metallicity star, while planet occurrence rises dramatically to $\sim 25\%$ for stars with three times the heavy metal composition of the Sun (Santos et al. 2005, Fischer & Valenti 2005). Ida & Lin (2004) have accounted for this metallicity correlation within the context of core accretion.

The statistical characteristics of exoplanets serve as tracers of planet formation and migration histories. The planet-metallicity correlation indicates initial high metallicity in the

protoplanetary disk which in turn may be correlated with a higher surface density of solid particles in the midplane of the disk that enhances core accretion. Orbital eccentricities and the proximity of gas giant planets to their host stars are remnant signatures of gravitational interactions that drive orbital migration. The architecture of multi-planet systems, sometimes locked in resonances, adds to our understanding of evolution of the protoplanetary disk.

The N2K program (Fischer et al. 2005) is a survey of metal-rich stars, designed to identify short period planets. These planets are geometrically endowed with a higher transit probability; transit events provide a rare opportunity to derive information about the planet density, internal structure and the atmosphere (Burrows et al. 2007, Charbonneau 2006, Sato et al. 2005). Because short-period planets can be flagged with just a few observations, the N2K program only requires three Doppler measurements to screen each star. However, an increased occurrence of planets is correlated with high host star metallicity at all detected separations. Therefore, additional observations were obtained for the highest metallicity stars to check for longer period planets. This extended program has detected six new intermediate period planets: HD 5319 and HD 75898 (Robinson et al. 2007), and four of the five planets presented here: HD 11506, HD 17156, HD 125612, HD 231701.

2. HD 11506

2.1. Stellar Characteristics

HD 11506 is classified as a G0 star with $V=7.51$. The Hipparcos catalog (ESA 1997) lists $B-V = 0.607$ with a parallax of 18.58 milliarcseconds, corresponding to a distance of 53.8 pc. The distance and apparent magnitude set the absolute visual magnitude as $M_V=3.85$ and the stellar bolometric luminosity as $2.29 L_\odot$, including a bolometric correction of -0.033 (VandenBerg & Clem 2003) based on effective temperature, surface gravity and metallicity of the star. High resolution spectroscopic analysis described in Valenti & Fischer (2005) yields $T_{\text{eff}} = 6058 \pm 51\text{K}$, $\log g = 4.32 \pm 0.08$, $v \sin i = 5.0 \pm 0.5 \text{ km s}^{-1}$, and $[\text{Fe}/\text{H}] = 0.31 \pm 0.03$ dex. HD 11506 is about 0.65 magnitudes above the main sequence. We expect the star to be located about 0.3 magnitudes above the main sequence because of high stellar metallicity, so this star appears to be slightly evolved by a few tenths of a magnitude, and is likely just beginning to transition onto the subgiant branch.

The stellar radius is calculated to be $1.3 R_\odot$ using $L = 4\pi R^2 \sigma T^4$. We have also run a fine grid of evolutionary tracks (described in Takeda et al. 2007), tuned to the uniform spectroscopic analysis of Valenti & Fischer (2005) and based on the Yale Stellar Evolution

Code. This analysis provides posterior probability distributions for stellar mass, radius, gravity and ages. Based on these evolutionary tracks, we derive a stellar mass of $1.19 M_{\odot}$, a radius of $1.38 R_{\odot}$, and an age of 5.4 Gyr. As a measure of the formal uncertainties, the lower and upper 95% credibility intervals from a Bayesian posterior probability distribution are provided in parentheses in Table 1 for these values.

The Ca II H & K lines (Figure 1) show that HD 11506 is chromospherically inactive. We measure S_{HK} , the core emission in the Ca II H & K lines relative to the continuum, for all of our stars. Based on nineteen Keck observations, we measure an average $S_{HK} = 0.156$ for HD 11506. The ratio of flux from S_{HK} to the bolometric stellar flux is designated as $\log R'_{HK}$ and gives the best diagnostic of chromospheric activity. The average $\log R'_{HK} = -4.99$ for this star and we derive an activity-based rotational period (Noyes et al. 1984), $P_{ROT} = 12.6d$, and an activity-based age of 5.4 Gyr, in excellent agreement with the age from evolutionary tracks. The activity, spectral type and evolutionary stage of the star allow us to estimate an additional source of astrophysical noise, or stellar jitter for the velocities of each of the stars on our Doppler survey (Wright 2005).

We monitored the brightness of HD 11506 with the T10 0.8 m automatic photometric telescope (APT) at Fairborn Observatory (Henry 1999, Eaton, Henry & Fekel 2003). The T10 APT measures the brightness of program stars relative to nearby constant comparison stars with a typical precision of 0.0015–0.0020 mag for a single measurement. For HD 11506, we obtained 102 b and y measurements spanning 451 days between 2004 October and 2006 January. The standard deviation of a single observation from the mean was 0.0023 mag, our upper limit to possible photometric variability in HD 11506. A periodogram analysis found no significant periodicity between 1 and 225 days, so our photometry confirms the star’s low chromospheric activity. The stellar parameters are summarized in Table 1.

2.2. Doppler Observations and Keplerian Fit

Doppler observations were made at the Keck telescope using HIRES (Vogt et al. 1994) with an iodine cell to model the instrumental profile and to provide the wavelength scale (Butler et al. 1996). An exposure meter maintains a constant signal-to-noise ratio of about 200 in our spectra, yielding a mean radial velocity precision of 2.75 m s^{-1} for HD 11506. We obtained a total of 26 Doppler measurements. The observation dates, radial velocities and measurement uncertainties for the radial velocities are listed in Table 2 and plotted in Figure 2.

In addition to velocity errors arising from our measurement uncertainties (including

photon shot noise), the star itself can have pulsations, cool spots or granular convective flows that contribute non-dynamical velocity noise. These astrophysical sources of noise are termed jitter and we empirically estimate stellar jitter based on the spectral type and chromospheric activity of the star, following Wright (2005). For purposes of fitting a Keplerian model, the stellar jitter is added in quadrature to the formal instrumental errors, however the estimated jitter is never included in the measurement uncertainties for the tabulated radial velocity sets.

The periodogram of the radial velocities shows a strong, broad peak in the power spectrum at about 1270 days with an associated false alarm probability (FAP) < 0.0001 . The FAP associated with the periodogram tests whether scrambled velocities yield power that exceeds the observed, unscrambled velocities. A high FAP suggests that the signal is not significant or could have been caused by a window function in the data. Using a Monte Carlo simulation, one thousand data sets of noise were generated by randomly drawing (with replacement) sets of actual stellar velocities. The fraction of trials with maximum periodogram power that exceeds the observed value from the initial unscrambled data set defines the FAP (Cumming 2004).

For each of the radial velocity data sets in this paper, a Levenberg-Marquardt fitting algorithm was used to model the radial velocities with a theoretical Keplerian orbital curve. There are six orbital parameters derived in the fit: orbital period (P), time of periastron passage (T_P), eccentricity (e), the orientation of the orbit (or line of apsides) (ω), the semi-velocity amplitude (K) and the residual center of mass radial velocity (after subtracting a median radial velocity).

Uncertainties in the orbital parameters are determined with a bootstrap Monte Carlo analysis. First, a best-fit Keplerian model is obtained. Then, for each of 100 trials, the theoretical best fit is subtracted from the observed radial velocities. The residual velocities are then scrambled (with replacement) and added back to the theoretical best fit velocities and a new trial Keplerian fit is then obtained. The standard deviation of each orbital parameter for the 100 Monte Carlo trials was adopted as the parameter uncertainty.

The best fit Keplerian model gives an orbital period of 1405 ± 45 d, semi-velocity amplitude of 80 ± 3 m s⁻¹ and orbital eccentricity of 0.3 ± 0.1 . The RMS to this fit is 10.8 m s⁻¹. Based on the chromospheric activity of this star, we estimated a jitter of 2 m s⁻¹ (Wright 2005). When this jitter is added in quadrature with the error bars listed in Table 2, $\sqrt{\chi^2_\nu} = 3.2$. While the large amplitude Doppler variation is clear, the $\sqrt{\chi^2_\nu}$ fit is worse than usual, suggesting that our velocity errors may be underestimated or that additional low amplitude dynamical velocities are present. A periodogram of the residual velocities to the single Keplerian fit show several peaks with similar power. For example, we

can fit a second planet with a period of 170 days with a significant reduction in the residual velocity RMS and an improvement in $\sqrt{\chi^2_\nu}$, however this is not yet a unique double planet fit; additional data are required to better evaluate the possible second signal.

Using the stellar mass of $1.19 M_\odot$ derived from evolutionary tracks, we find $M \sin i = 4.74 M_{\text{JUP}}$ and a semi-major axis of 2.48 AU. At the distance of this star, this physical separation corresponds to an angular separation of $\alpha = 0.''04$. The Keplerian orbital solution is listed in Table 3 and the best-fit Keplerian model is plotted in Figure 2.

3. HD 17156

3.1. Stellar Characteristics

HD 17156 is listed as a G5 star in the SIMBAD database and the Hipparcos catalog. However, this spectral type seems at odds with other data for the star. The visual magnitude is $V = 8.17$, $B - V = 0.59$, and the Hipparcos parallax (ESA 1997) is 12.78 milliarcseconds, corresponding to a distance of 78.24 pc. The bolometric correction -0.039 (VandenBerg & Clem 2003) and absolute visual magnitude, $M_V = 3.70$, imply a bolometric stellar luminosity of $2.6 L_\odot$. Spectroscopic analysis yields $T_{\text{eff}} = 6079 \pm 56\text{K}$, $\log g = 4.29 \pm 0.06$, $v \sin i = 2.6 \pm 0.5 \text{ km s}^{-1}$, and $[\text{Fe}/\text{H}] = 0.24 \pm 0.03$. The $B - V$ color and the effective temperature are independent measurements that are consistent with each other. Together with the absolute magnitude and position on the H-R diagram, the spectral type for this star is more likely to be G0 and the star is just beginning to evolve off the main sequence.

The stellar mass, from evolutionary models described by Takeda et al. (2007), is $1.2 M_\odot$, and the age is 5.7 Gyr. The stellar radius from evolutionary models is $1.47 R_\odot$, and agrees with the value we derive using the observed luminosity and the Stefan-Boltzmann relation.

The absence of Ca II H & K emission (Figure 1) demonstrates low chromospheric activity. Taking the average of 25 observations, we measure $S_{HK} = 0.15$ and $\log R'_{HK} = -5.04$ and derive a rotational period, $P_{ROT} = 12.8 \text{ d}$, with an estimated stellar age of $6.4 \pm 2 \text{ Gyr}$, which compares favorably with the age derived above from stellar evolution tracks.

We obtained 241 photometric measurements with the T12 APT spanning 179 days between 2006 September and 2007 March. The standard deviation of the observations from their mean was 0.0024 mag, the upper limit to photometric variability in the star. Periodogram analysis revealed no significant periodicity between 1 and 100 days. In particular, a least-squares sine fit of the observations on the 21.22-day radial velocity period resulted

in a photometric amplitude of only 0.00039 ± 0.00023 mag, providing further evidence that the radial velocity variations in HD 17156 are not due to chromospheric activity. The stellar characteristics, including our assessment of photometric variability, are summarized in Table 1.

3.2. Doppler Observations and Keplerian Fit

We initially obtained eight Doppler observations of HD 17156 using the High Dispersion Spectrometer (Noguchi et al. 2002) at the Subaru Telescope in 2004 and 2005. For the first observing runs, the iodine absorption cell was located behind the entrance slit of the spectrometer (Kambe et al. 2002, Sato et al. 2002, Sato et al. 2005). The box holding the I2 cell included a window with a lens to maintain constant focal length inside the spectrometer. This eliminated the need to adjust the collimator position when moving the I2 cell in and out of the light path (i.e., when taking program and template observations). However, the lens introduced a different wavelength dispersion for program observations relative to the template observation. Modeling of those early data is still ongoing, however, standard stars, known to have constant radial velocities show RMS scatter greater than 15 m s^{-1} , with larger run-to-run velocity offsets for Doppler observations obtained with that setup.

The Subaru N2K program was awarded ten nights of “intensive” time in summer 2006 and in December 2006. Before the intensive time allocation, the iodine cell was moved in front of the slit, eliminating the change in wavelength dispersion between template and program observations. With this new setup, the RMS scatter decreased, ranging from 4 - 12 m s^{-1} in a set of four RV standard stars.

HD 17156 had exhibited large radial velocity variations in 2004 - 2005 at Subaru. Follow-up observations at Keck confirmed velocity variations, so the star was observed on nine consecutive nights at Subaru from 8 December to 16 December, 2006. Setup StdI2b was used to cover the wavelength region of 3500–6100 Å with a mosaic of two CCDs. The slit width of $0''.6$ was used to give a reciprocal resolution ($\lambda/\Delta\lambda$) of 60000. We obtained a typical signal-to-noise ratio of $S/N \sim 150 \text{ pixel}^{-1}$ at 5500 Å with exposure times of about 120 seconds. Because of the larger systematic errors for observations taken before summer 2006 (with the iodine cell behind the slit), only the nine radial velocities from December 2006 are listed in Table 4. To account for the intrinsic RMS velocity scatter in standard stars, 5 m s^{-1} was added in quadrature to the nine Subaru observations in Table 4.

After HD 17156 was flagged as an N2K candidate at Subaru, it was added to the N2K planet search program at Keck. We obtained 24 radial velocity measurements at the

Keck Observatory with an average internal velocity precision of 1.6 m s^{-1} . Observation dates, radial velocities and uncertainties for 33 observations are listed in Table 4. The last column designates the source of the observations as “K” (Keck Observatory) or “S” (Subaru Observatory). The periodogram of the radial velocity data shows a strong narrow peak at 21.1 days with a FAP less than 0.0001 (for 10000 Monte Carlo trials).

When combining the Subaru and Keck velocities, we first determined a velocity difference of about 130 m s^{-1} between two observations taken at Subaru and Keck on the same night (JD 2454083.9). With that initial guess, we included a velocity offset as a free parameter and found that an offset of 116.0 m s^{-1} produced a minimum $\sqrt{\chi^2_\nu}$. That offset was added to the Subaru velocities listed in Table 4. The best fit Keplerian model for the combined Subaru and Keck data sets yields an orbital period of $21.2 \pm 0.3 \text{ d}$, semi-velocity amplitude, $K = 275 \pm 15 \text{ m s}^{-1}$, and orbital eccentricity, $e = 0.67 \pm 0.08$. The RMS to the fit is 3.97 m s^{-1} . Adding jitter of 3 m s^{-1} (expected for this star) in quadrature with the actual single-measurement errors gives $\sqrt{\chi^2_\nu} = 1.04$ for this Keplerian fit.

Adopting a stellar mass of $1.2 M_\odot$, we derive $M \sin i = 3.12 M_{\text{JUP}}$ and a semi-major axis of 0.15 AU. The Keplerian orbital solution is summarized in Table 3. The phase-folded plot of the Doppler measurements for Keck and Subaru observations are shown in the left plot of Figure 3 and include 3 m s^{-1} jitter. Keck observations are represented by diamonds and the Subaru observations are shown as filled circles.

Because the high eccentricity is unusual, we examined the Keplerian fit for the Keck data alone, shown in the right plot Figure 3. The Keck data have poor phase coverage near periastron, and yield a Keplerian fit with lower amplitude and lower eccentricity. The Subaru observations map periastron passage and help to model the eccentricity of the orbit.

3.3. Transit Search

The 21.22 day period of the companion to HD 17156 is by far the shortest planetary orbital period in this paper. The orbital semi-major axis of 0.15 AU and the stellar radius of $1.47 R_\odot$ lead to an *a priori* transit probability of 7% (Seagroves et al. 2003). Therefore, we used our 241 brightness measurements to conduct a preliminary transit search. The orbital parameters in Table 3 constrain the predicted times of transit to about ± 0.3 days, which is slightly greater than the 0.25-day duration of a central transit. We performed our transit search, using a technique similar to the one described by Laughlin (2000), over all orbital phases for periods between 20 and 23 days. The search was negative but was able to cover effectively only 25% of the period-phase search space corresponding to the uncertainties in

the orbital parameters. Thus, our photometric data do not preclude the possibility of transits in HD 17156.

4. HD 125612

4.1. Stellar Characteristics

HD 125612 is a G3V main sequence star with $V=8.31$, $B-V = 0.628$, and Hipparcos parallax (ESA 1997) of 18.93 corresponding to a distance of 52.82 pc and absolute visual magnitude, $M_V=4.69$. Spectroscopic analysis yields $T_{\text{eff}} = 5897 \pm 40\text{K}$, $\log g = 4.45 \pm 0.05$, $v \sin i = 2.1 \pm 0.5 \text{ km s}^{-1}$, and $[\text{Fe}/\text{H}]= 0.24 \pm 0.03$ dex. The bolometric correction is -0.061, giving a stellar luminosity of $1.08 L_{\odot}$. The luminosity and T_{eff} imply a stellar radius of $1.0 R_{\odot}$. Within uncertainties, this agrees well with the value of $1.05 R_{\odot}$ determined from stellar evolutionary tracks. We also derive a stellar mass of $1.1 M_{\odot}$ from stellar evolution models and an age of 2.1 Gyr.

Figure 1 shows the Ca H line for HD 125612; the lack of emission indicates low chromospheric activity for this star. Taking the mean of 18 observations, we measure $S_{HK} = 0.178$ and $\log R'_{HK} = -4.85$, and derive $P_{ROT} = 10.5$ d, and a stellar age of 3.3 ± 2 Gyr (which compares well with the age of 2.1 Gyr from stellar evolution tracks). Stellar parameters are summarized in Table 1.

4.2. Doppler Observations and Keplerian Fit

We obtained 19 Keck velocity measurements for HD 125612 with a typical uncertainty of 2.2 m s^{-1} . Observation dates, radial velocities and instrumental uncertainties in the radial velocities are listed in Table 5. A periodogram of the velocities shows a strong broad peak at about 500 days.

The best fit Keplerian model is plotted in Figure 4 and yields a period of 510 ± 14 d, with semi-velocity amplitude $90.7 \pm 8 \text{ m s}^{-1}$, orbital eccentricity, 0.38 ± 0.05 , and a linear trend of 0.037 meters per day. Adopting a stellar mass of $1.1 M_{\odot}$, we derive $M \sin i = 3.5 M_{\text{JUP}}$ and semi-major axis of 1.2 AU (angular separation, $\alpha = 0''.023$). The Keplerian orbital solution is listed in Table 3 and the RV data are plotted with the best-fit Keplerian model (solid line) in Figure 4.

The RMS to the Keplerian fit shown in Figure 4 is 10.7 m s^{-1} . The velocity jitter for this star is expected to be about 2 m s^{-1} . Therefore, the residual RMS is several times

the typical error bar, consistent with the poor $\sqrt{\chi^2_\nu}$ statistic of 3.56. A periodogram of the residuals to a 510-day planet fit shows power near 3.5 d. However, there are several other peaks of nearly comparable height, showing that other orbital solutions may give similar improvements. Thus, while we could fit the residuals with a second Keplerian, the FAP of the peak does not yet meet our standards of statistical significance, and more data are required for follow up.

5. HD 170469

5.1. Stellar Characteristics

HD 170469 is a G5 subgiant star with visual magnitude $V=8.21$, $B-V = 0.677$, and Hipparcos parallax (ESA 1997) of 15.39 milliarcseconds, corresponding to a distance of 64.97 pc. The absolute visual magnitude of the star is $M_V=4.14$. The bolometric correction is -0.072 providing a bolometric stellar luminosity of $1.6 L_\odot$ and (with T_{eff}) stellar radius of $1.2 R_\odot$ calculated from the luminosity. Evolutionary tracks provide a stellar mass estimate of $1.14 M_\odot$ and stellar radius of $1.22 R_\odot$ and age of 6.7 Gyr. Our spectroscopic analysis gives $T_{\text{eff}} = 5810 \pm 44\text{K}$, $\log g = 4.32 \pm 0.06$, $v \sin i = 1.7 \pm 0.5 \text{ km s}^{-1}$, and $[\text{Fe}/\text{H}] = 0.30 \pm 0.03$ dex.

The Ca H & K lines (Figure 1) indicate low chromospheric activity. Taking the mean of thirteen observations, we measure $S_{HK} = 0.145$ and $\log R'_{HK} = -5.06$ and derive a rotational period, $P_{ROT} = 13.0$ d and an activity-calibrated age (Noyes et al. 1984) of 7 ± 2 Gyr.

We obtained 215 brightness measurements with the T10 APT spanning 630 days between 2005 March and 2006 November. The standard deviation of the observations was 0.0018 mag, the upper limit to photometric variability in HD 170469. A periodogram analysis found no significant periodicity between 1 and 315 days, confirming the star's low chromospheric activity. The stellar characteristics are summarized in Table 6.

5.2. Doppler Observations and Keplerian Fit

We obtained 35 Keck velocities for HD 170469 with a mean velocity precision of 1.6 m s^{-1} . Observation dates, radial velocities and instrumental uncertainties in the radial velocities are listed in Table 7. A periodogram of the velocities yields very strong power at about 1100 days with a FAP less than 0.0001.

The best fit Keplerian model gives an orbital period of 1145 ± 18 d, semi-velocity

amplitude of $12.0 \pm 1.9 \text{ m s}^{-1}$ and orbital eccentricity, 0.11 ± 0.08 . The RMS to the fit is 4.18 m s^{-1} with $\sqrt{\chi^2_\nu} = 1.59$, including the estimated astrophysical jitter of 2.0 m s^{-1} . Adopting a stellar mass of $1.14 M_\odot$, we derive $M \sin i = 0.67 M_{\text{JUP}}$ and a semi-major axis of 2 AU ($\alpha = 0.''03$). The Keplerian orbital parameters are listed in Table 8 and the RV data are plotted with the best-fit Keplerian model (solid line) in Figure 5.

6. HD 231701

6.1. Stellar Characteristics

HD 231701 is an F8V star with $V = 8.97$, $B - V = 0.539$, and Hipparcos parallax (ESA 1997) of 9.22 milliarcseconds, corresponding to a distance of 108.4 pc. The absolute visual magnitude is $M_V = -3.79$, so this star is beginning to evolve onto the subgiant branch. Spectroscopic analysis yields $T_{\text{eff}} = 6208 \pm 44\text{K}$, $\log g = 4.33 \pm 0.06$, $v \sin i = 4.0 \pm 0.5 \text{ km s}^{-1}$, and $[\text{Fe}/\text{H}] = 0.07 \pm 0.03$ dex. The bolometric correction is -0.037 and bolometric luminosity is $2.4 L_\odot$. The luminosity and effective temperature yield a stellar radius of $1.36 R_\odot$. Modeling the stellar evolutionary tracks, we derive a stellar mass of $1.14 M_\odot$, radius of $1.35 R_\odot$, and age of 4.9 Gyr.

The Ca H&K lines (Figure 1) show that the star has low chromospheric activity. We measure $S_{\text{HK}} = 0.159$ and $\log R'_{\text{HK}} = -5.0$ and derive a rotational period, $P_{\text{ROT}} = 12.2 \text{ d}$ and a stellar age of $5.6 \pm 2 \text{ Gyr}$. Stellar parameters are listed in Table 6.

6.2. Doppler Observations and Keplerian Fit

We obtained 17 Keck observations of HD 231701 with mean internal errors of 3.2 m s^{-1} . Observation dates, radial velocities and measurement uncertainties in the radial velocities are listed in Table 9. The periodogram of this data set has a FAP of 0.006 for a period near 140 days.

The best fit Keplerian model has an orbital period of $141.6 \pm 2.8 \text{ d}$, with semi-velocity amplitude $39 \pm 3.5 \text{ m s}^{-1}$ and orbital eccentricity, 0.1 ± 0.06 . The RMS to this fit is 5.9 m s^{-1} . The expected astrophysical jitter for this star is 2.2 m s^{-1} . Adding this jitter in quadrature with the error bars listed in Table 9 yields $\sqrt{\chi^2_\nu} = 1.46$ for this Keplerian fit. Adopting the stellar mass of $1.14 M_\odot$, we derive $M \sin i = 1.08 M_{\text{JUP}}$ and semi-major axis of 0.53 AU. The Keplerian orbital solution is listed in Table 8 and the phased RV data is plotted with the best-fit Keplerian model (solid line) in Figure 6.

6.3. Discussion

Here, we present the detection of 5 new exoplanets detected with Doppler observations. For each of the Keplerian models, we also carried out a Markov Chain Monte Carlo (MCMC) analysis to better estimate the orbital parameters and their uncertainties following the algorithm described by Ford (2003). Unlike the Levenberg-Marquardt algorithm that we generally use to determine a best fit Keplerian orbit, the MCMC analysis provides the full posterior probability density distribution for each parameter. This approach is particularly useful for data sets where the Levenberg-Marquardt algorithm can minimize $\sqrt{\chi^2_\nu}$ with a model that fits a sparse data set. The MCMC algorithm explores a wider range of parameter space because it is not driven solely by $\sqrt{\chi^2_\nu}$ minimization. However, MCMC does not explore an exhaustive range of parameter space. For example, solutions with very different orbital periods might be missed. For each of the models presented here, we began with the input parameters found with Levenberg Marquardt fitting and confirmed that the orbital elements were recovered with strongly peaked probability distributions using MCMC.

HD 170469 is a star on the regular planet search at Keck that has a planet of $M \sin i = 0.66 M_{\text{JUP}}$ in a ~ 3 yr orbit with eccentricity 0.23. The host star is metal-rich with $[\text{Fe}/\text{H}] = 0.3$. The remaining four exoplanets were initially part of the N2K program at Keck. The N2K program targets metal-rich stars for rapid identification of short-period planets. The first three radial velocity measurements for the stars presented here had RMS scatter less than 5 m s^{-1} (except HD 17156, with initial RMS scatter of 34 m s^{-1}), so these stars were not candidates for short period planets. However, a follow-up program to obtain Doppler observations on N2K-vetted high metallicity stars with low chromospheric activity and low RMS velocity scatter has detected the presence of these longer period planets.

HD 11506 b is a fairly massive planet, with $M \sin i = 4.74 M_{\text{JUP}}$ and a semi-major axis of 2.5 AU. This could well constitute the outer edge of a habitable zone location for putative rocky moons orbiting the planet, depending on atmospheric properties of any moons. The host star has a luminosity that is 2.3 times that of the Sun. The eccentricity of this system is 0.3, so the temperature at the top of the planet atmosphere would change by about 50K between apastron and periastron.

HD 17156 b has a mass of $M \sin i = 3.12 M_{\text{JUP}}$ and an orbital period of 21.2 days, placing it in the so-called period valley between 10 and 100 days (Udry et al. 2003), where a relatively small fraction of exoplanets have been detected. We derive a substantial orbital eccentricity of 0.67 for HD 17156 b. At this proximity to the subgiant host star, the planet moves between 0.05 and 0.25 AU, experiencing temperature changes of a few hundred degrees between periastron and apastron. It is possible that these thermal changes could be observed with sensitive IR flux measurements from space, even though the planet is not known to

transit its host star.

The distribution of orbital eccentricities for known exoplanets is shown in Figure 7. An upper envelope in the distribution of eccentricities rises steeply from periods of a few days to reach the maximum observed eccentricities (for HD 80606 and HD 20782) at periods of 100 - 1000 days. Although an orbital eccentricity of 0.67 seems remarkable for HD 17156 b, given its orbital period of just 21.2 days, the eccentricity still falls along the upper edge of the observed eccentricity distribution.

HD 125612 b has $M \sin i = 3.5 M_{\text{JUP}}$ with a semi-major axis of 1.2 AU. This planet has an eccentricity of 0.38. The planet is carried from 0.47 AU at periastron, where the temperature at the top of the atmosphere is about 300 K, to about 2.1 AU where the temperature falls below the freezing point of water to about 200 K. A single planet model does not appear to adequately describe the velocities of HD 125612 because the RMS to that fit is 10.7 m s^{-1} , yet the star is chromospherically quiet and slowly rotating, with $v \sin i = 2 \text{ km s}^{-1}$. This star may well have an additional planet orbiting in a relatively short period.

Velocity variations in HD 231701 have been modeled as a planet with $M \sin i = 1.08 M_{\text{JUP}}$ with a semi-major axis of 0.53 AU and orbital eccentricity of about 0.1. The MCMC probability distributions for HD 231701 are consistent with this Keplerian model, but allow for eccentricity solutions that extend to zero. This analysis alerts us that more RV measurements should be taken to better constrain the orbital eccentricity of this system.

We have now obtained three or more Doppler observations for 423 stars at Keck Observatory as part of the N2K program. Spectral synthesis modeling has been carried out for all of these stars, and we plot the percentage of stars with detected planets in each 0.1 dex metallicity bin in Figure 8. Superimposed on this plot is the planet detectability curve from Fischer & Valenti (2005). A planet probability can be assigned based on the stellar metallicity. Integrating planet probabilities we expect 27 ± 5 exoplanets with masses greater than $1 M_{\text{JUP}}$ and orbital periods shorter than 4 years. Fourteen, or about half of the expected planets in the sample have now been detected.

We gratefully acknowledge the dedication and support of the Keck Observatory staff, in particular Grant Hill for support with HIRES. We thank Akito Tajitsu and Tae-Soo Pyo for their expertise and support of the Subaru HDS observations. DAF acknowledges support from NASA grant NNG05G164G and from Research Corporation. SSV acknowledges support from NSF AST-0307493. BS is supported by Grants-in-Aid for Scientific Research (No. 17740106) from the Japan Society for the Promotion of Science (JSPS). We thank the Michelson Science Center for travel support through the KPDA program. We thank the NASA and UC Telescope assignment committees for generous allocations of telescope

time. The authors extend thanks to those of Hawaiian ancestry on whose sacred mountain of Mauna Kea we are privileged to be guests. Without their kind hospitality, the Keck observations presented here would not have been possible. This research has made use of the SIMBAD database, operated at CDS, Strasbourg, France, and of NASA’s Astrophysics Data System Bibliographic Services and is made possible by the generous support of Sun Microsystems, NASA, and the NSF.

REFERENCES

- Butler, R. P., Wright, J. T., Marcy, G. W., Fischer, D. A., Vogt, S. S., Tinney, C. G., Jones, H. R. A., Carter, B. D., Johnson, J. A., McCarthy, C., Penny, A. J. 2006 *ApJ* 646, 505
- Butler, R. P., Marcy, G. W., Williams, E., McCarthy, C., Dosanji, P., Vogt, S. S. 1996, *PASP*, 108, 500
- Burrows, A., Hubeny, I., Budaj, J., Hubbard, W. 2007, *ApJ*, in press
- Charbonneau, D., Brown, T. M., Burrows, A., Laughlin, G. 2006, in *Protostars and Planets V*, ed. B. Reipurth, D. Jewitt, and K. Keil (University of Arizona Press)
- Cumming, A. 2004, *MNRAS*, 354, 1165
- Eaton, J. A., Henry, G. W., Fekel, F. C. 2003, in *The Future of Small Telescopes in the New Millennium, Volume II—The Telescopes We Use*, ed. T. D. Oswalt (Dordrecht: Kluwer), 189
- ESA 1997, *The Hipparcos and Tycho Catalogs*. ESA-SP 1200
- Fischer, D. A. et al. 2005, *ApJ*, 629, 481
- Fischer, D. A., Valenti, J. A. 2005, *ApJ* 622, 1102
- Ford, E. 2003, *ApJ*, 129, 1706
- Henry, G. W. 1999, *PASP*, 111, 845
- Laughlin, G. 2000, *ApJ*, 545, 1064
- Ida, S., Lin, D. N. C. 2004, *ApJ* 616, 567
- Kambe, E. et al. 2002, *PASJ*, 54, 873
- Marcy, G. W., Butler, R. P., Fischer, D. A., Vogt, S. S., Wright, J. T., Tinney, C. G., Jones, H. R. A. 2005, *PThPS*, 158, 24
- Noguchi, K. et al. . 2002, *PASJ*, 54, 855
- Noyes, R. W., Hartmann, L., Baliunas, S. L., Duncan, D. K., Vaughan, A. H. 1984, *ApJ*, 279, 763
- Robinson, S. E., Laughlin, G., Vogt, S. S., Fischer, D., Butler, R. P., Marcy, G. W., Takeda, G., Driscoll, P. 2007, *ApJ* in press
- Santos, N. C., Israelian, G., Mayor, M., Bento, J. P., Almeida, P. C., Sousa, S. G., Ecuivillon, A. 2005, *A & A*, 437, 1127
- Sato, B., Kambe, E., Takeda, Y., Izumiura, H., Ando, H. 2002, *PASJ*, 54 873
- Sato, B. et al. 2005, *ApJ*, 633, 465
- Seagroves, S., Harker, J., Laughlin, G., Lacy, J., & Castellano, T. 2003, *PASP*, 115, 1355
- Takeda, G., Ford, E. B., Sills, A., Rasio, F., Fischer, D. A., Valenti, J. A. 2007, *ApJS*, 168, 297

- Udry, S., Mayor, M., Clausen, J. V., Freyhammer, L. M., Helt, B. E., Lovis, C., Naef, D., Olsen, E. H., Pepe, F., Queloz, D., Santos, N. C. 2003, *A & A*, 407, 679
- Valenti, J. A., Fischer, D. A. 2005, *ApJS*, 159, 141
- VandenBerg, D. & Clem, J. 2003, *AJ*, 126, 778
- Vogt, S. S. et al. 1994, *SPIE*, 2198, 362.
- Wright, J. T. 2005, *PASP*, 117, 657
- Wright, J. T., Marcy, G. W., Fischer, D. A., Butler, R. P., Vogt, S. S., Tinney, C. G., Jones, H. R. A., Carter, B. D., Johnson, J. A., McCarthy, C., Apps, K. 2007, *ApJ*, 657, 533

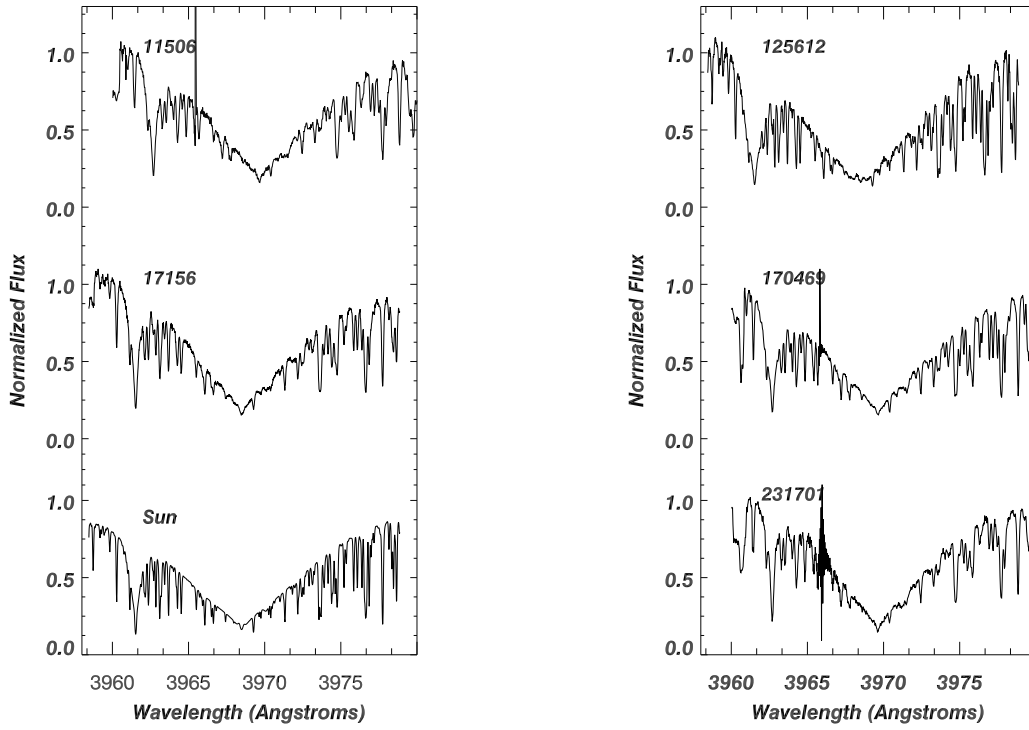


Fig. 1.— The Ca H line for HD 11506 and 17156 are plotted in the left panel, with the same wavelength segment of the Sun shown for comparison. HD 125612, HD 170469 and HD 231701 are plotted in the right panel. All of these stars have low chromospheric activity based on our measurement of line core emission relative to the continuum.

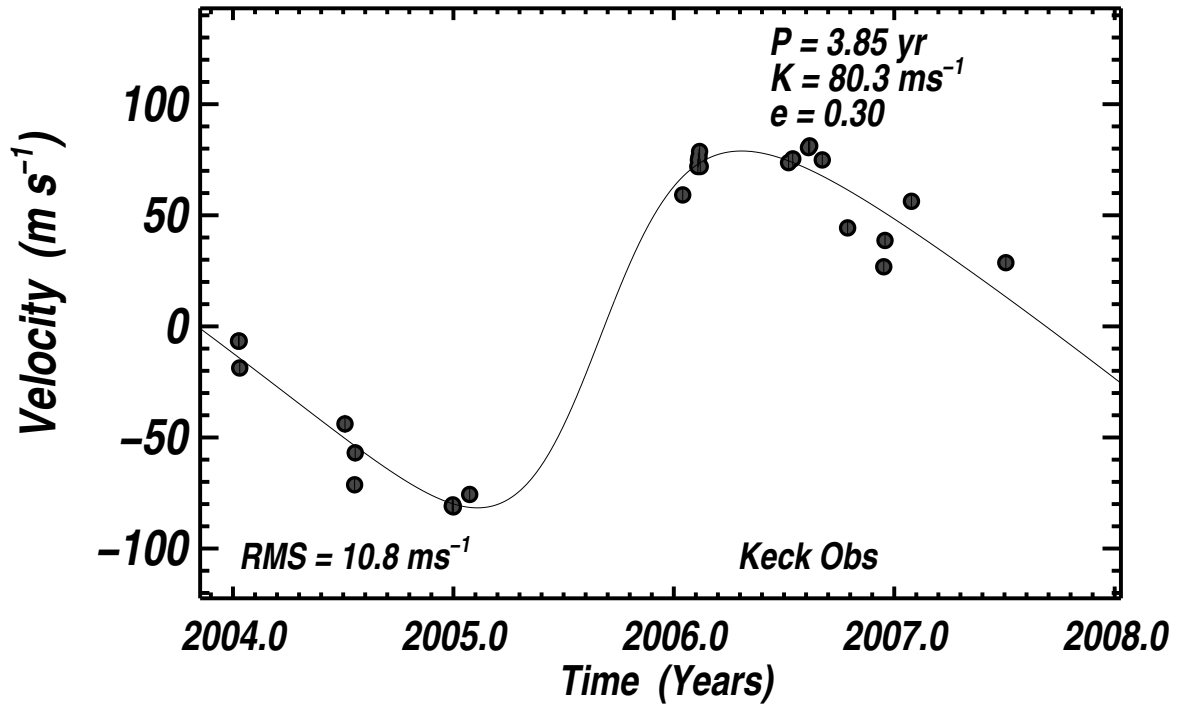


Fig. 2.— Radial velocities for HD 11506. The velocity error bars have been augmented by adding 2 m s^{-1} in quadrature to the single measurement precision listed in Table 2. This gives $\sqrt{\chi^2_\nu} = 3.2$ for the Keplerian fit. With a stellar mass of $1.19 M_\odot$, we derive a planet mass of $M \sin i = 4.74 M_{\text{JUP}}$ and semi-major axis, $a_{\text{rel}} = 2.48 \text{ AU}$.

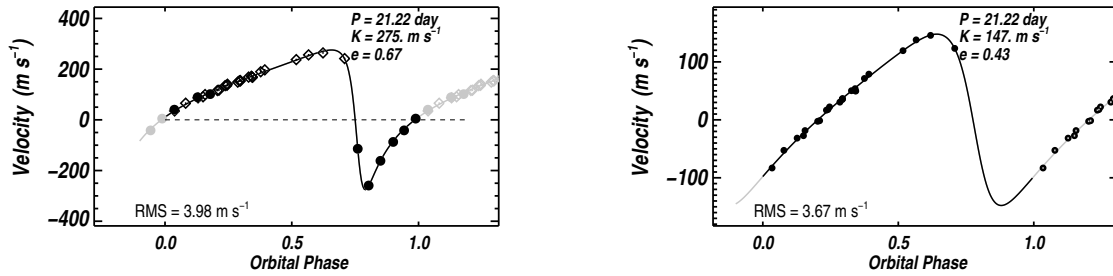


Fig. 3.— (left) Radial velocities for HD 17156 from Keck Observatory (diamonds) and Subaru Observatory (filled circles) have 3 m s^{-1} added in quadrature to the uncertainties listed in Table 4 to account for expected photospheric jitter. Adopting a stellar mass of $1.2 M_{\odot}$ we derive a planet mass, $M \sin i = 3.12 M_{\text{JUP}}$ and semi-major axis for the orbit, $a_{\text{rel}} = 0.15 \text{ AU}$. (right) The plot on the right shows the Keck velocities only. Although the phase coverage misses periastron the Keck velocities alone confirm high eccentricity in HD 17156 b.

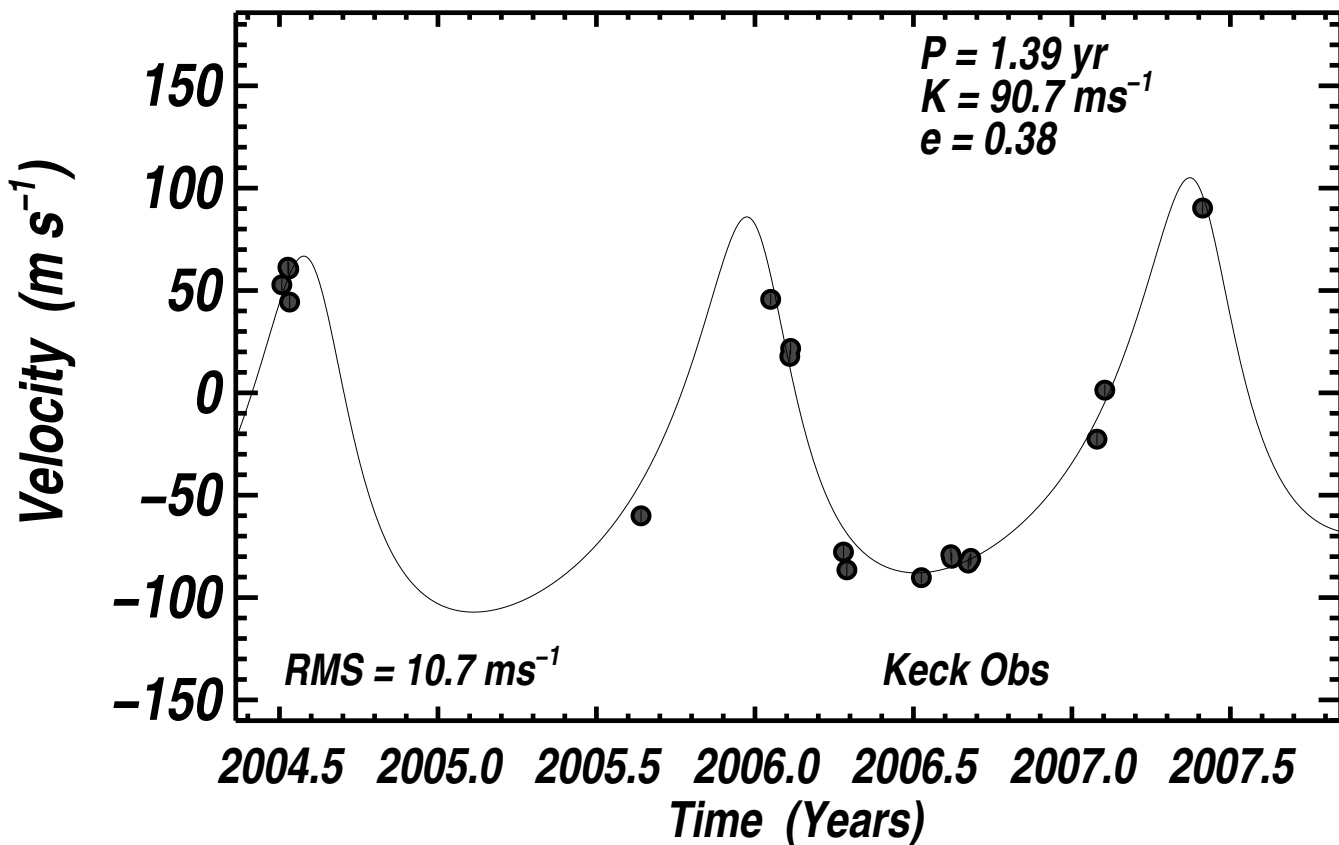


Fig. 4.— Radial velocities for HD 125612. The velocity measurements have 2 m s^{-1} added to their error bars listed in Table 5 to account for the level of astrophysical noise (jitter) we expect from the star. With the assumed stellar mass of $1.1 M_{\odot}$, we derive a planet mass, $M \sin i = 3.5 M_{\text{JUP}}$ and semi-major axis of 1.2 AU. This Keplerian model still has a high RMS and $\sqrt{\chi^2_{\nu}}$ of 3.56, suggesting the possible presence of an additional planet.

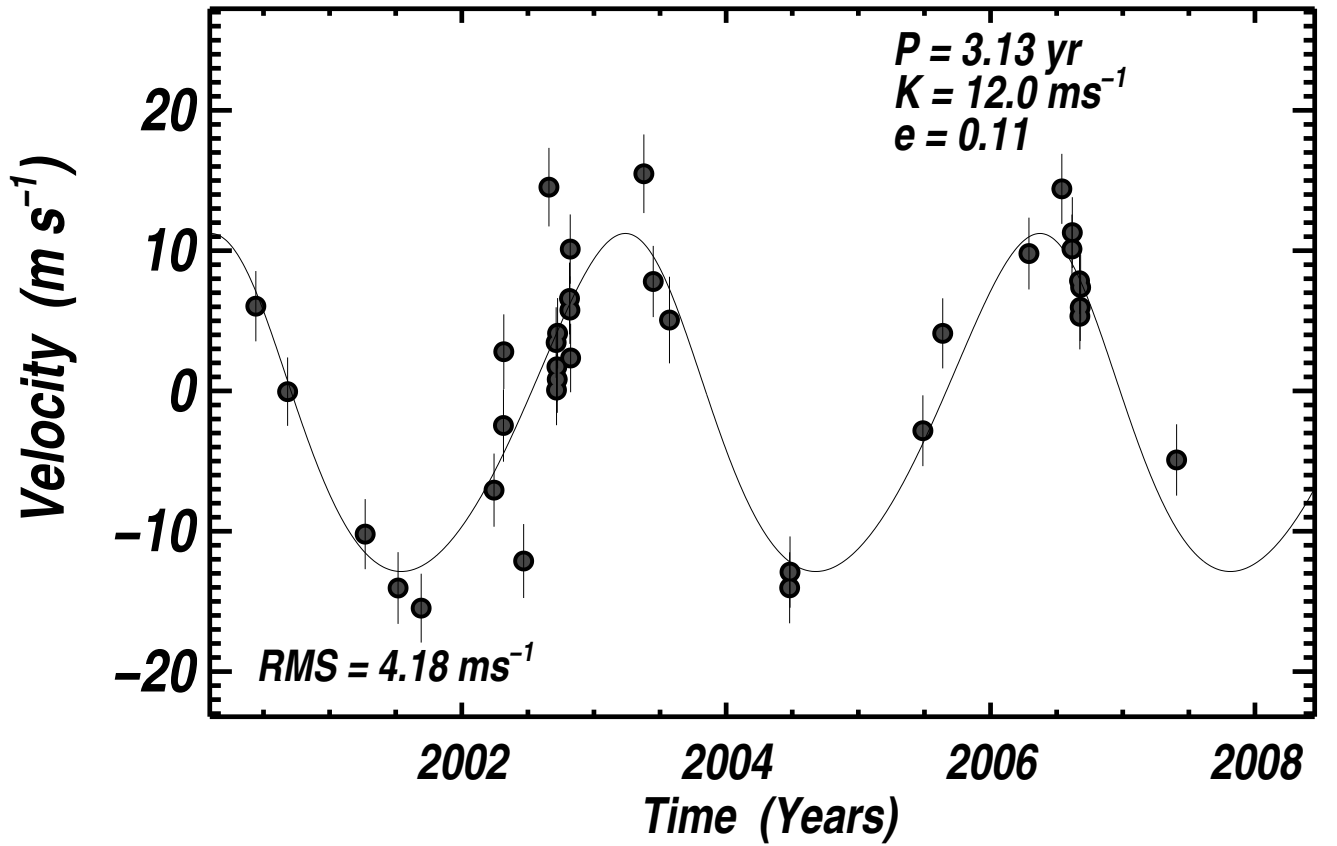


Fig. 5.— Keck radial velocities for HD 170469 include 2.0 m s^{-1} added in quadrature with the internal error bars listed in Table 7. With the added jitter, the Keplerian fit has $\sqrt{\chi^2_\nu} = 1.59$. The assumed stellar mass of $1.14 M_\odot$ yields a planet mass of $M \sin i = 0.67 M_{\text{JUP}}$ and semi-major axis of about 2 AU.

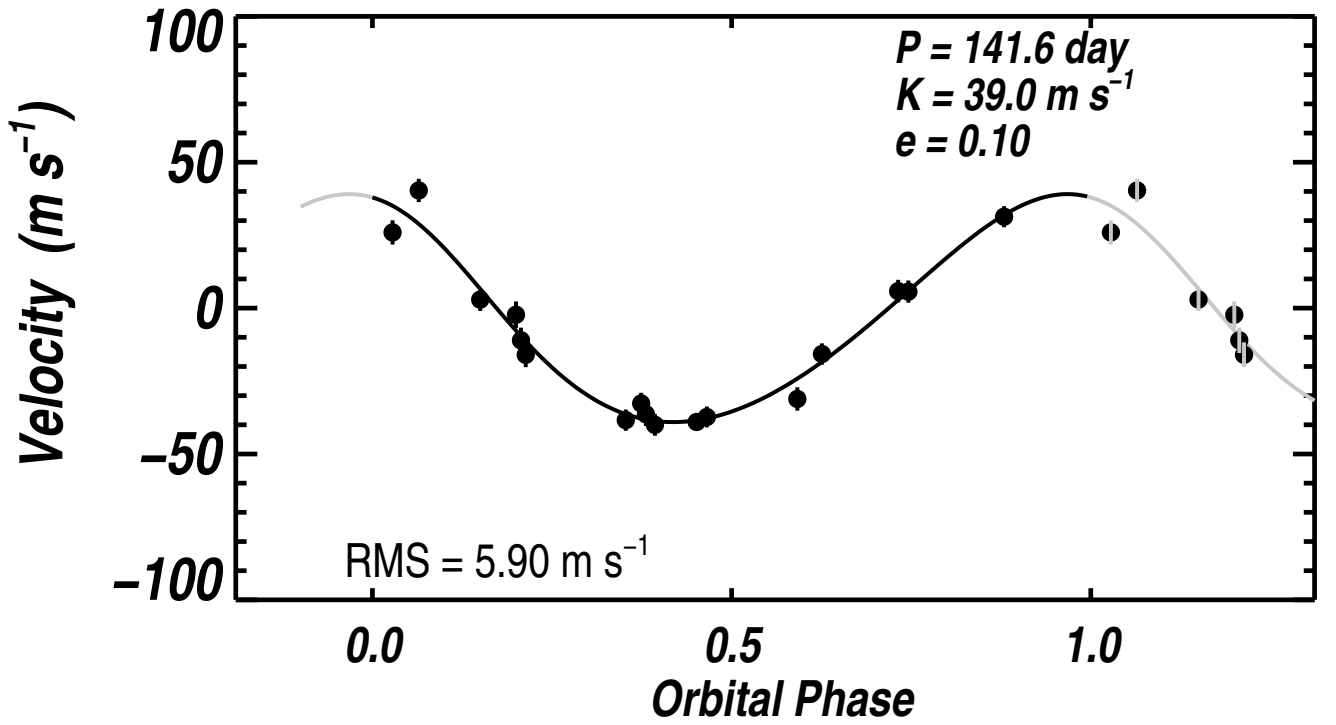


Fig. 6.— Phase-folded radial velocities for HD 231701 include stellar jitter of 2.2 m s⁻¹ added to the errors listed in Table 9, giving $\sqrt{\chi^2_{\nu}} = 1.46$. The stellar mass of $1.14 M_{\odot}$ implies a planet mass of $M \sin i = 1.08 M_{\text{JUP}}$ and orbital radius of 0.53 AU.

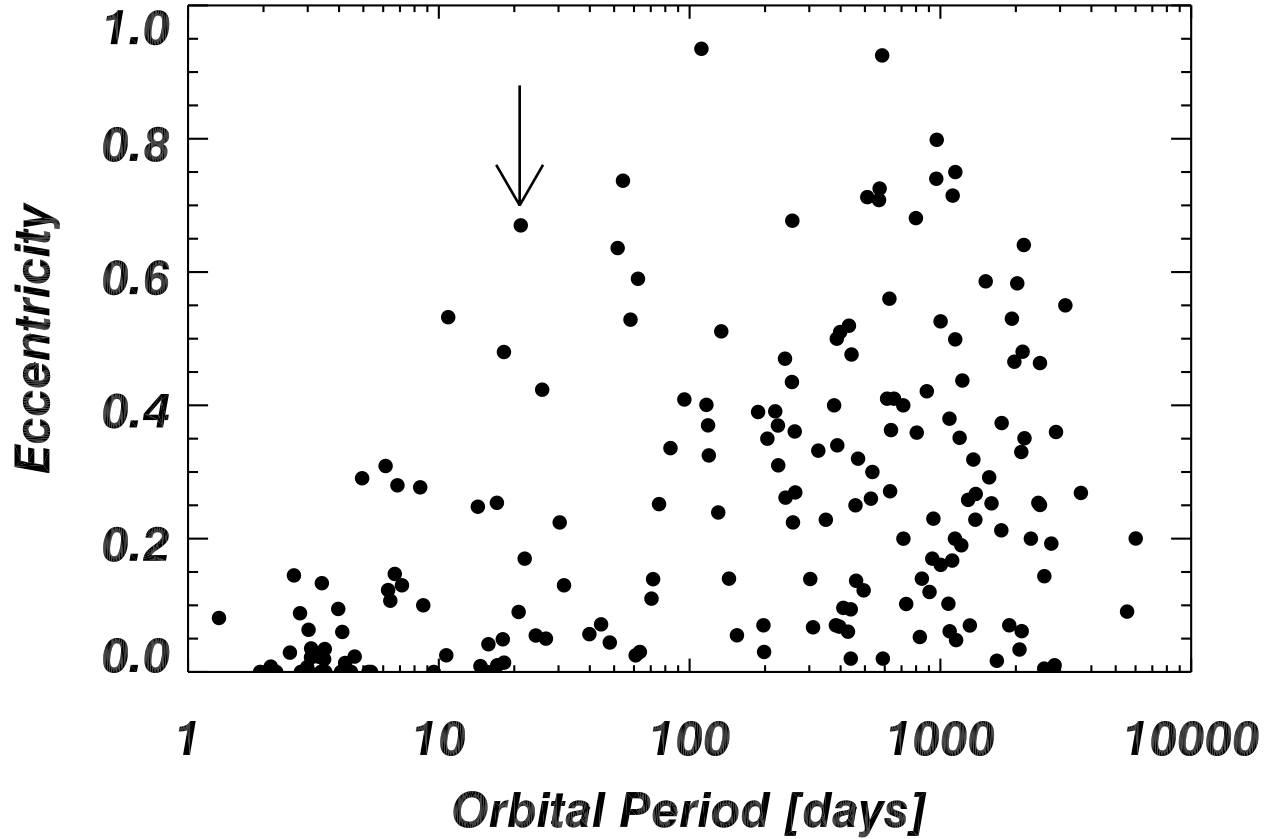


Fig. 7.— Orbital eccentricity distribution for exoplanets. A rising envelope defines the distribution for planets with periods between 2 and 100 days. The distribution peaks for periods between 100 - 1000 days. The arrow points to the dot representing HD 17156 b. With an orbital period of 21 days and eccentricity of 0.67, HD 17156 b still fits within the envelope of this eccentricity distribution.

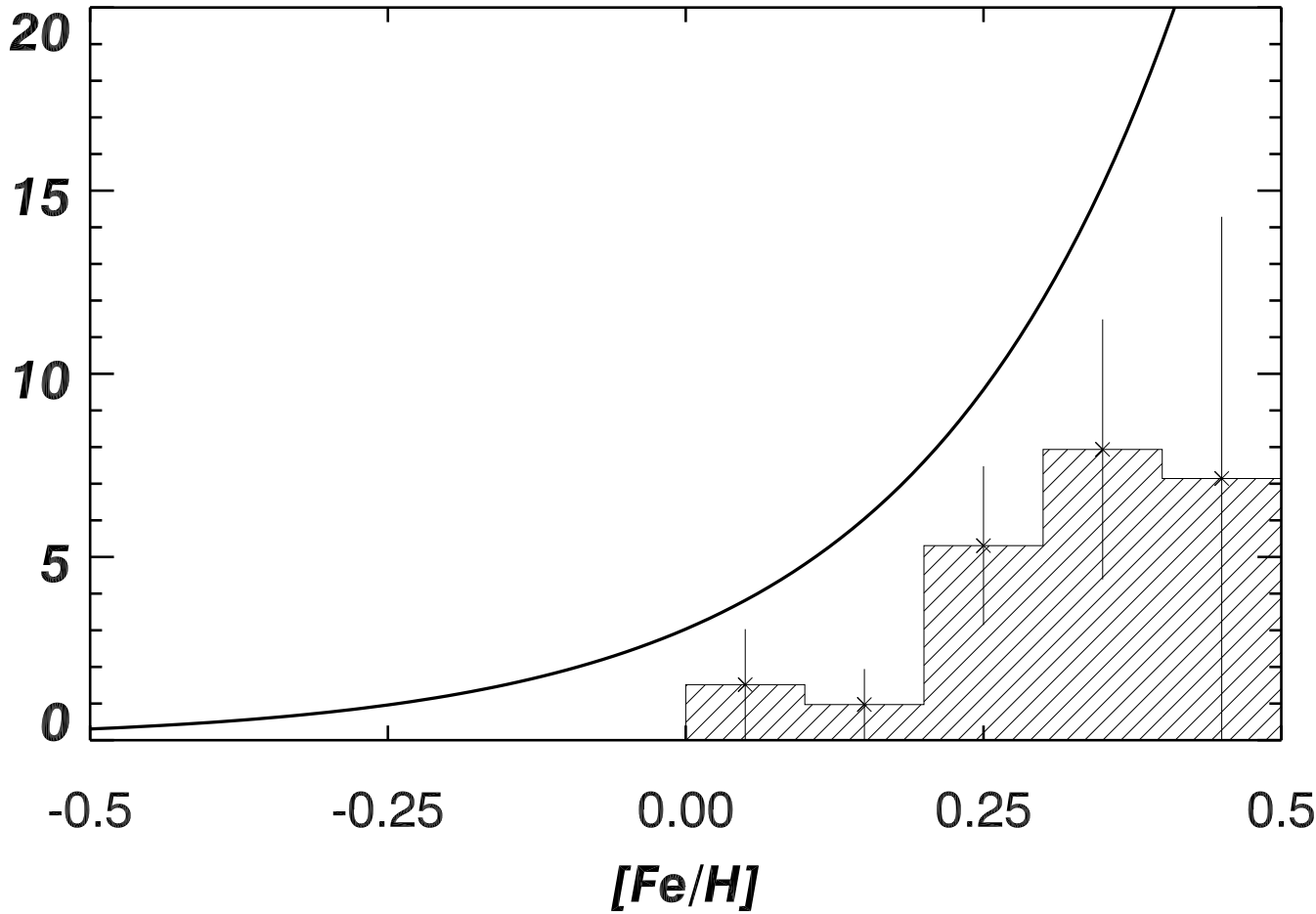


Fig. 8.— Stars with at least 4 Doppler observations that were observed at Keck as part of the N2K program were binned according to metallicity. In each 0.1 dex metallicity bin, the percentage of stars with detected planets is plotted and Poisson error bars are shown. Superimposed on this histogram is the curve of planet occurrence as a function of metallicity from Fischer & Valenti (2005). Most stars on the N2K program have only 4-5 observations, however the metallicity correlation is still emerging and is supported in this sample.

Table 1. Stellar Parameters

Parameter	HD11506	HD17156	HD125612
V	7.51	8.17	8.31
M_V	3.85	3.70	4.69
B-V	0.607	0.590	0.628
Spectral Type	G0V	G0V	G3V
Distance (pc)	53.82	78.24	52.82
L_{bol}/L_{\odot}	2.29	2.6	1.08
[Fe/H]	0.31 (0.03)	0.24 (0.03)	0.24 (0.03)
T_{eff} (K)	6058 (51)	6079 (56)	5897 (40)
$v \sin i$ (km s ⁻¹)	5.0 (0.50)	2.6 (0.50)	2.1 (0.50)
log g	4.32 (0.08)	4.29 (0.06)	4.45 (0.05)
M_{STAR} (M_{\odot}) ^a	(1.1) 1.19 (1.29)	(1.1) 1.2 (1.3)	(1.04) 1.1 (1.17)
R_{STAR} (R_{\odot}) ^a	(1.25) 1.38 (1.53)	(1.3) 1.47 (1.6)	(0.99) 1.05 (1.13)
Age (Gyr) ^a	(3.9) 5.4 (7.0)	(3.8) 5.7 (7.0)	(0.16) 2.1 (5.6)
S_{HK}	0.156	0.15	0.178
log R'_{HK}	-4.99	-5.04	-4.85
P_{ROT} (d)	12.6 d	12.8 d	10.5 d
σ_{phot} (mag)	0.0023	0.0024	...

^aStellar masses, radii and ages are derived from evolutionary tracks

Table 2. Radial Velocities for HD 11506

JD -2440000.	RV (m s ⁻¹)	Uncertainties (m s ⁻¹)
13014.73505	-6.67	2.94
13015.73893	-6.58	2.89
13016.74089	-18.73	2.98
13191.12201	-43.89	3.56
13207.10116	-71.30	3.17
13208.08401	-56.92	3.41
13368.83778	-80.87	2.26
13369.75897	-80.35	2.18
13370.73242	-81.24	2.17
13397.73009	-75.66	2.36
13750.73807	59.16	2.67
13775.72853	71.94	2.77
13776.70435	74.90	2.57
13777.72528	76.27	2.93
13778.71858	78.70	2.73
13779.74737	71.93	2.77
13926.12744	73.68	2.66
13933.09065	75.37	2.62
13959.13935	80.47	2.46
13961.12421	81.24	2.73
13981.98256	74.91	3.12
14023.97438	44.32	3.07
14083.84327	26.82	2.44
14085.92115	38.66	2.54
14129.74332	56.29	2.48
14286.11838	28.66	3.01

Table 3. Orbital Parameters

Parameter	HD 11506	HD 17156	HD 125612
P (d)	1405 (45)	21.2 (0.3)	510 (14)
T _p (JD)	13603 (102)	13738.529 (0.5)	13228.3 (12)
ω (deg)	262 (19)	121 (11)	21 (9)
ecc	0.3 (0.1)	0.67 (0.08)	0.38 (0.05)
K ₁ (m s ⁻¹)	80 (3)	275 (15)	90.7 (8)
dv/dt (m s ⁻¹ per day)	0.037
a_{rel} (AU)	2.48	0.15	1.2
$a_1 \sin i$ (AU)	0.0099	0.00039	0.0039
$f_1(m)$ (M _☉)	6.53e-08	1.83e-08	3.09e-08
$M \sin i$ (M _{Jup})	4.74	3.12	3.5
Nobs	26	33	19
RMS (m s ⁻¹)	10.8	3.97	10.7
Jitter (m s ⁻¹)	2	3	2
Reduced $\sqrt{\chi^2_\nu}$	3.2	1.17	3.56
FAP (periodogram)	< 0.0001	< 0.0001	0.0003

Table 4. Radial Velocities for HD 17156

JD -2440000.	RV (m s ⁻¹)	Uncertainties (m s ⁻¹)	Observatory
13746.75596	88.49	1.70	K
13748.79814	138.15	1.73	K
13749.79476	151.35	1.67	K
13750.80160	169.65	1.76	K
13775.77821	235.17	1.83	K
13776.80791	253.80	1.81	K
13779.82897	239.14	1.64	K
13959.13219	97.33	1.55	K
13962.07028	152.64	1.51	K
13963.10604	165.48	1.68	K
13964.13118	194.69	1.70	K
13982.03231	132.55	1.20	K
13983.08575	146.35	1.70	K
13983.99480	166.11	1.32	K
13985.00847	187.22	1.57	K
14023.95206	114.39	1.77	K
14047.95773	166.01	1.74	K
14078.01162	-116.60	5.14	S
14078.92501	-261.56	5.18	S
14079.91371	-164.10	5.23	S
14080.98093	-89.57	5.13	S
14081.89406	-44.08	5.15	S
14082.86071	2.39	5.14	S
14083.88445	37.62	5.16	S
14083.90314	32.76	1.33	K
14084.82860	63.22	1.63	K
14085.82560	86.67	5.20	S
14085.86537	84.28	1.56	K
14086.87960	99.01	5.20	S

Table 4—Continued

JD -2440000.	RV (m s ⁻¹)	Uncertainties (m s ⁻¹)	Observatory
14129.92513	113.30	1.43	K
14130.73019	133.66	1.32	K
14131.85485	151.11	1.77	K
14138.76720	261.56	1.37	K

Table 5. Radial Velocities for HD 125612

JD -2440000.	RV (m s ⁻¹)	Uncertainties (m s ⁻¹)
13190.83262	52.80	2.85
13197.83363	61.40	2.66
13198.85557	60.49	2.59
13199.83792	44.35	2.70
13604.75480	-60.07	2.04
13754.12824	45.68	1.83
13776.15380	17.80	2.03
13777.11940	21.71	2.16
13838.01492	-77.76	2.35
13841.94894	-86.49	2.52
13927.79007	-90.28	2.01
13961.75080	-79.07	2.01
13962.74127	-80.81	1.83
13981.72862	-83.16	1.90
13983.74037	-81.92	2.11
13984.72815	-80.88	2.03
14130.13392	-22.62	2.18
14139.12383	1.31	1.94
14251.82778	90.28	2.39

Table 6. Stellar Parameters

Parameter	HD 170469	HD 231701
V	8.21	8.97
M_V	4.14	3.79
B-V	0.677	0.539
Spectral Type	G5IV	F8V
Distance (pc)	64.97	108.4
L_{bol}/L_\odot	1.6	2.4
[Fe/H]	0.30 (0.03)	0.07 (0.03)
T_{eff} (K)	5810 (44)	6208 (44)
$v \sin i$ (km s ⁻¹)	1.7 (0.5)	4 (0.50)
log g	4.32 (0.06)	4.33 (0.06)
M_{STAR} (M_\odot) ^a	(1.05) 1.14 (1.16)	(1.08) 1.14 (1.22)
R_{STAR} (R_\odot) ^a	(1.15) 1.22 (1.3)	(1.16) 1.35 (1.55)
Age (Gyr) ^a	(5.0) 6.7 (7.8)	(3.5) 4.9 (6.2)
S_{HK}	0.145	0.159
log R'_{HK}	-5.06	-5.00
P_{ROT} (d)	13.0 d	12.2 d
σ_{phot} (mag)	0.0018	...

^aStellar masses, radii and ages are derived from evolutionary tracks

Table 7. Radial Velocities for HD 170469

JD -2440000.	RV (m s ⁻¹)	Uncertainties (m s ⁻¹)
11705.96808	6.04	1.51
11793.81330	-0.05	1.39
12008.04881	-10.21	1.50
12099.03294	-14.05	1.59
12162.76894	-15.48	1.42
12364.13287	-7.07	1.67
12390.12499	-2.46	1.63
12391.12567	2.80	1.76
12445.93867	-12.12	1.72
12515.82777	14.53	1.96
12535.75539	3.45	1.53
12536.74191	0.06	1.50
12537.82520	1.72	1.50
12538.74254	0.83	1.30
12539.75501	4.11	1.51
12572.69435	6.59	1.60
12573.69333	5.76	1.34
12574.70725	10.11	1.45
12575.69822	2.35	1.40
12778.04455	15.48	1.96
12804.05044	7.80	1.56
12848.92274	5.06	2.35
13180.90825	-14.03	1.55
13181.89752	-12.91	1.57
13548.99248	-2.83	1.54
13603.80234	4.11	1.50
13842.01212	9.79	1.59
13932.96654	14.41	1.49
13960.91798	10.12	1.42

Table 7—Continued

JD	RV	Uncertainties
-2440000.	(m s ⁻¹)	(m s ⁻¹)
13961.83115	11.29	1.54
13981.82421	7.85	1.27
13982.77494	5.33	1.26
13983.76067	5.96	1.33
13984.83377	7.38	1.22
14250.01196	-4.92	1.57

Table 8. Orbital Parameters

Parameter	HD 170469	HD 231701
P (d)	1145 (18)	141.6 (2.8)
T _p (JD)	11669.0 (21)	13180.0 (4.2)
ω (deg)	34 (19)	46 (24)
ecc	0.11 (0.08)	0.10 (0.08)
K ₁ (m s ⁻¹)	12.0 (1.9)	64 (8)
dv/dt (m s ⁻¹ per day)
a_{rel} (AU)	2.1	0.53
$a_1 \sin i$ (AU)	0.00126	0.0005
$f_1(m)$ (M _⊙)	2.03e-10	8.6e-10
$M \sin i$ (M _{Jup})	0.67	1.08
Nobs	35	17
RMS (m s ⁻¹)	4.18	5.90
Jitter (m s ⁻¹)	2.0	2.22
Reduced $\sqrt{\chi^2_\nu}$	1.59	1.46
FAP (periodogram)	< 0.0001	0.006

Table 9. Radial Velocities for HD 231701

JD -2440000.	RV (m s ⁻¹)	Uncertainties (m s ⁻¹)
13190.98047	1.98	3.41
13198.03808	-2.44	4.00
13199.02309	-11.19	3.74
13199.95689	-16.16	3.62
13603.87134	40.18	3.32
13928.04498	-38.57	2.90
13931.08095	-32.84	2.93
13932.02123	-36.55	3.38
13961.87814	-31.29	3.34
13981.76292	5.66	3.18
13983.77988	5.49	3.11
14023.71873	25.79	3.53
14083.69519	-39.18	2.43
14085.70009	-37.48	2.83
14217.13510	-40.18	2.99
14250.07410	-15.89	2.90
14286.00169	31.17	2.86